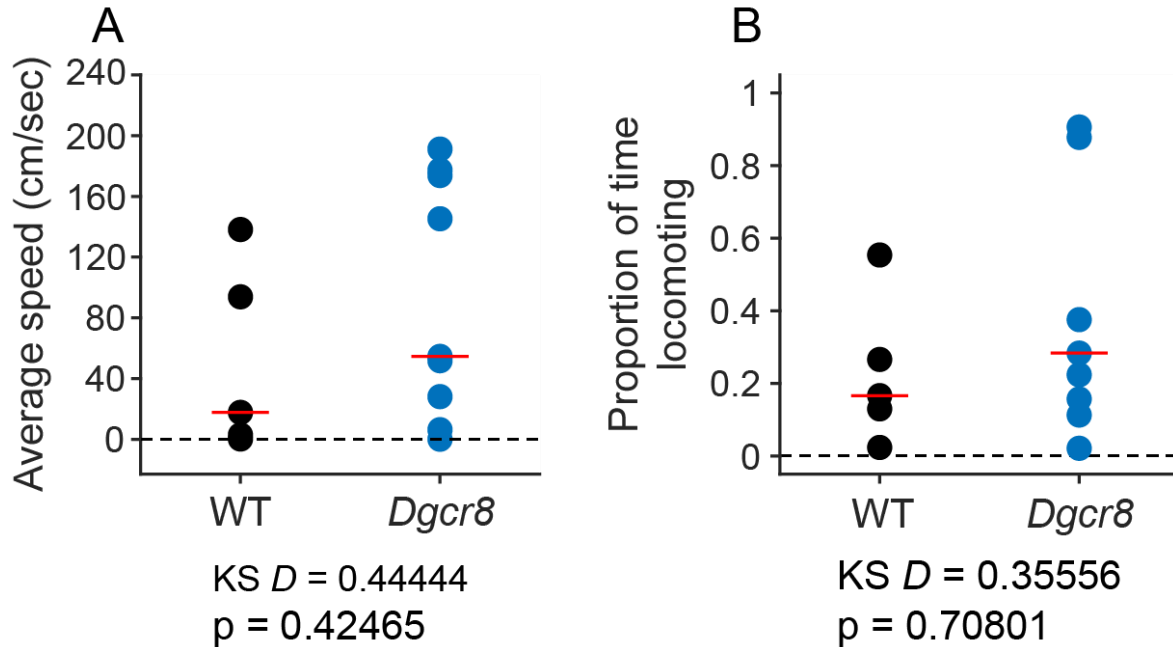
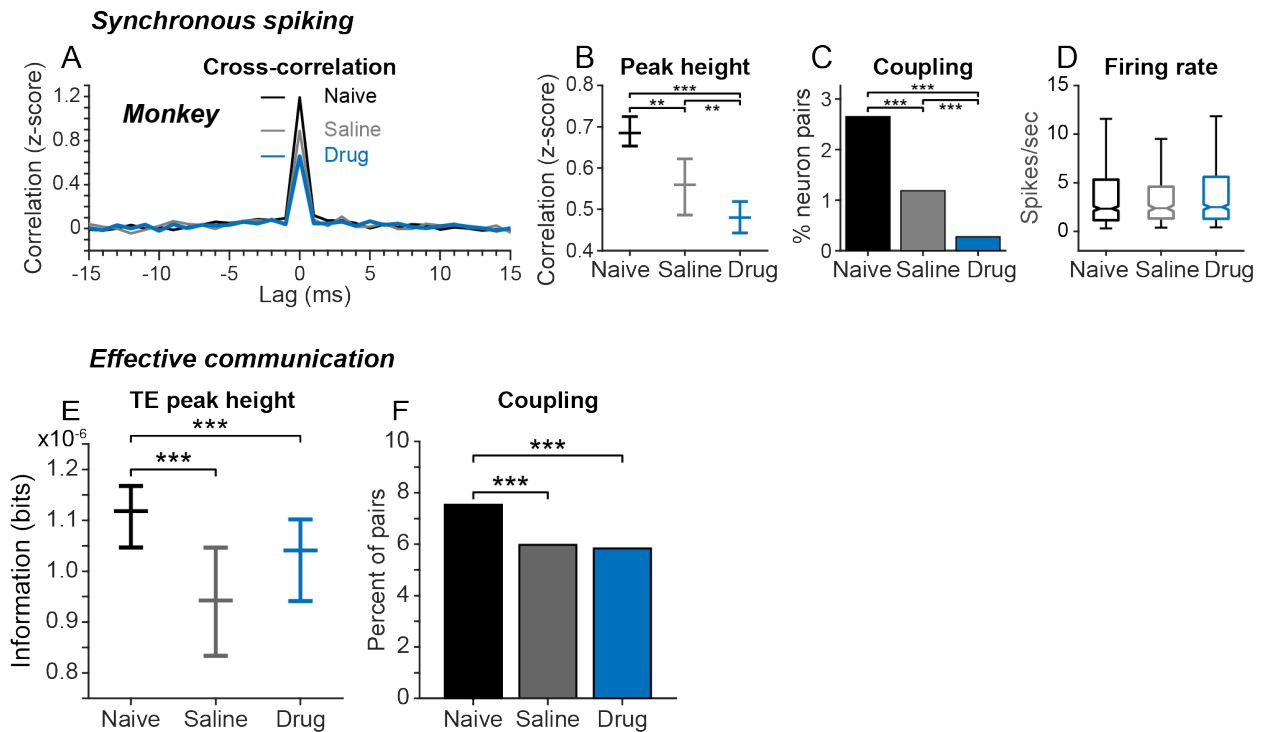


### Locomotion in WT and *Dgcr8* mice



**Figure S1. Locomotion in mice during neural recording sessions did not vary by genotype. Related to Figures 2 and 3.** A rotary encoder was employed to generate a signal for each 1/4 of a turn of the running wheel, which had diameter = 14.6 cm and circumference = 45.9 cm. **A.** Average speed of wheel movement by mice during recording sessions in cm/sec, separated by genotype (WT or *Dgcr8*). Red lines represent the median value within genotype. There was no significant difference by group on a two-sided Kolmogorov-Smirnov test (KS statistic = 0.44,  $p = 0.42$ ; red lines represent the median value within genotype). **B.** Proportion of time during the recording session during which the mouse was actively locomoting, separated by genotype (WT or *Dgcr8*). There was no significant difference by group on a two-sided Kolmogorov-Smirnov test (KS statistic = 0.36,  $p = 0.71$ ).

## Intermittent NMDAR antagonism persistently disrupts prefrontal circuit dynamics



**Figure S2. Persistent changes in prefrontal circuit dynamics following intermittent NMDAR antagonist exposure. Related to Figures 2 and 3.** We recorded neural data in monkey prefrontal cortex first in the Naive condition (before initiating the regimen of daily NMDAR antagonist injections), and then following interleaved daily injections of either NMDAR antagonist (Drug condition) or saline (Saline condition). **A-D.** Comparison of 0-lag spike synchrony across Naive, Saline and Drug conditions. The height of the CCH 0-lag peak in the Saline condition was intermediate between 0-lag peak heights in the Naive and Drug conditions (A, B; Kruskal-Wallis test between Naive, Saline, and Drug conditions;  $X^2_{df=2} = 83.4$ ,  $p < 10^{-19}$ ,  $N_{\text{Naive}} = 7,393$  pairs,  $N_{\text{Saline}} = 2,443$  pairs,  $N_{\text{Drug}} = 6,165$  pairs; pairwise comparisons by Tukey HSD test,  $**p < 0.01$ ;  $***p < 0.001$ ). The percentage of neuron pairs exhibiting a significant CCH 0-lag peak in the Saline condition was similarly intermediate between the percentages seen in the Naive and Drug conditions (two-tailed z test of proportions,  $**p < 0.01$ ;  $***p < 0.001$ ). These changes in spike timing were seen without concurrent changes in neuronal firing rate between Naive, Saline and Drug conditions (D; Kruskal-Wallis test,  $p = 0.32$ ), **E, F.** Comparison of TE functional communication between neurons in the Naive, Saline and Drug conditions. The TE peak was significantly lower in both the Saline and Drug conditions relative to the Naive condition (E; Kruskal-Wallis test,  $X^2_{df=2} = 27.8$ ,  $p < 10^{-6}$ ,  $N_{\text{Naive}} = 14,702$  directional pairs, e.g. considering TE from neuron A→B and also B→A,  $N_{\text{Saline}} = 4,870$  directional pairs,  $N_{\text{Drug}} = 12,320$  directional pairs; pairwise comparisons by Tukey HSD test;  $***p < 0.001$ ). The percentage of neuron pairs exhibiting significant peaks was lower in both the Saline and Drug conditions relative to the Naive condition also (F; two-tailed z test of proportions,  $**p < 0.01$ ;  $***p < 0.001$ ). Saline and Drug conditions did not significantly differ relative to one another with respect either to the height of the TE peak or the proportion of neuron pairs exhibiting significant TE peaks.

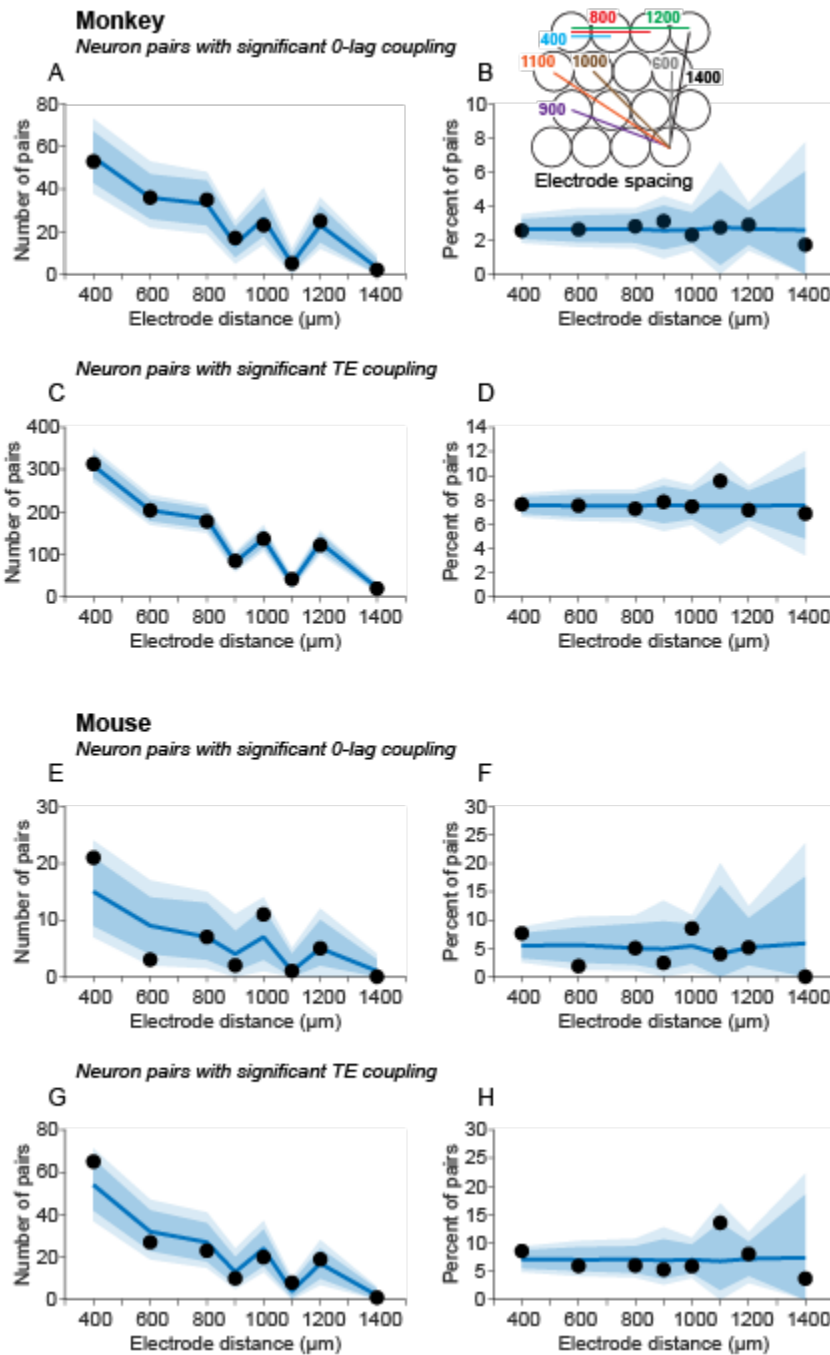


**Figure S3. Neuronal 0-lag and TE coupling as a function of electrode distance. Related to Figures 2 and 3.** We examined whether the proportion of neuron pairs exhibiting significant 0-lag spike synchrony or TE functional coupling varied as a function of the distance between the electrodes on which the neurons were recorded. Neuron pairs recorded on the same electrode were excluded, and only neuron pairs recorded under control conditions (drug naïve in monkey, WT in mouse) were included in pairwise analyses. Electrodes were spaced at 400 microns in a regular 4 x 4 grid (Panel B inset), and pairs of electrodes in the array were spaced at one of eight distances in the range of 400-1400  $\mu\text{m}$ . Filled circles in each panel indicate the total number of

neuron pairs (left column; A, C, E, G) and percent of recorded neuron pairs (right column; B, D, F, H) at each interelectrode distance that exhibited significant CCH 0-lag or TE peaks. Dark blue shaded regions illustrate the 5th and 95th percentiles, (and light blue shaded regions illustrate the 0.5th and 99.5th percentiles) of a bootstrap distribution of corresponding neuron pair numbers and percentages at each distance generated by randomly shuffling interelectrode distances between neuron pairs (1000 iterations). The bulk of neuron pairs in our sample were recorded on pairs of electrodes at the nearer distances in this range. Correspondingly, we observed more neuron pairs exhibiting significant 0-lag spike synchrony and TE coupling recorded on electrodes that were less than 800  $\mu\text{m}$  apart in both monkeys and mice (A, C, E, G). However, relative to all neurons recorded at each distance, the proportion of neuron pairs exhibiting significant 0-lag spike synchrony or TE coupling did not vary significantly as a function of the distance between the electrodes on which the neurons were recorded in the range we sampled, either in monkeys (B, D; 0-lag,  $\chi^2 = 1.72$ ,  $p = 0.97$ ; TE,  $\chi^2 = 3.61$ ,  $p = 0.82$ ), or mice (F, H; 0-lag,  $\chi^2 = 11.66$ ,  $p = 0.11$ ; TE,  $\chi^2 = 10.31$ ,  $p = 0.17$ ). Across both monkey and mouse datasets, there were no counts of pairs (A, C, E, G) nor percent of pairs (B, D, F, H) that fell outside of the 5% false discovery cutoff (corrected for multiple comparisons) of respective bootstrap distributions.

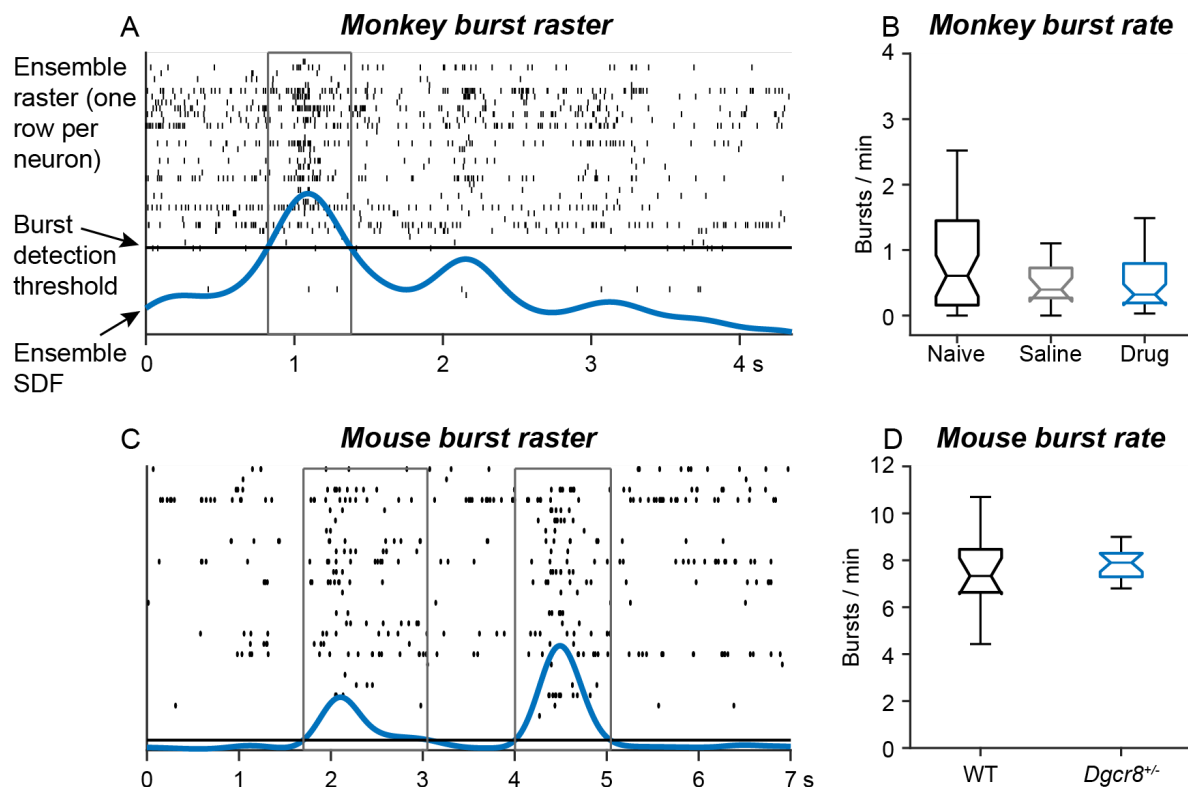


**Figure S4. Bursting activity in monkey and mouse prefrontal neurons. Related to Figures 2 and 3.** **A, C.** Tick marks indicate the times of action potentials. Rows are different neurons. The blue line is the normalized ensemble spike density function (SDF). The black horizontal line is the burst detection threshold. Thin vertical lines delimit periods of ensemble bursting detected by the algorithm (ensemble SDF > threshold). **A.** Example raster illustrating the activity of a neural ensemble in monkey prefrontal cortex in the Naive condition. **B.** Distribution of burst rates in monkey prefrontal cortex by drug condition. The median burst rate across ensembles did not

significantly differ between the Naive (0.6 min<sup>-1</sup>), Saline (0.4 min<sup>-1</sup>), and Drug (0.3 min<sup>-1</sup>) conditions (Kruskal-Wallis test,  $p = 0.37$ ). **C.** Example raster illustrating the activity of a neural ensemble in mPFC of a wildtype mouse. **D.** Distribution of burst rates in mouse prefrontal cortex by genotype. The median burst rate across ensembles did not significantly differ between WT (7.3 min<sup>-1</sup>) and Dgcr8<sup>+/-</sup> animals (7.9 min<sup>-1</sup>) (Kruskal-Wallis test,  $p = 0.28$ ).